

B. Hancock

Pfizer Global Research and Development, Groton, CT 06340 USA

M. Dutt

Department of Materials Science and Metallurgy, University of Cambridge, Cambridge CB1 7XE, UK

C. Bentham

Pfizer Global Research and Development, Sandwich, Kent CT13 9NJ, UK

J. Elliott

Department of Materials Science and Metallurgy, University of Cambridge, Cambridge CB1 7XE, UK

We study a system of monodisperse frictional particles confined between two surfaces and being simultaneously sheared and uniaxially compacted by the upper surface. The upper surface is made of particles identical to those in the bulk, arranged randomly, or in a square or triangular lattice. The particles between the surfaces are allowed to compact under gravity after being poured onto the bottom surface, followed by simultaneous constant strain compaction and shear by the upper surface. We focus on the evolution of the packing structure with interparticle friction, arrangements of the particles on the surfaces, initial height of the confined gravitationally compacted particles and the shear and compaction strain rates. We compute the coordination number, packing fraction, contact orientation, distribution of contacts and other relevant quantities to provide quantitative insight on the packing structure. We have found, for a 5 diameter layer of confined particles, the compaction speed has a greater effect on the packing structure of the particles in comparison to the shear speed. For a shearing surface formed of particles arranged in a square lattice, the packing structure of the confined particles evolves to interdigitating layers of 3D close-packed spheres. The numerical experiments have been performed via Discrete Element Method simulations (Dutt et al., 2004 submitted) using Microcrystalline Cellulose spheres.

1 INTRODUCTION

Constant strain compaction of granular materials (Jaeger, Nagel & Behringer 1996) from a perspective of particle packing, has extensive applications, for example, the generation of detergent or pharmaceutical tablets (Alderborn & Nystrom 1996). Insight into the process can be obtained by studying the evolution of the particle packing structure (Richard, Phillippe, Barbe, Bourles, Thibault & Bideau 2003) or the pore structure; the two being intimately related. Compaction will constrain the particle motion along the direction of application, causing plastic deformations, or slipping of the particles at the interparticle contacts, to fill up the neighboring voids. The hypothetical question we ask is whether a strain applied simultaneously, normal to the compaction direction, influences the void filling process. The additional shear strain will drag the particles in contact with the shearing sur-

face, allowing them to explore the neighboring interstices and translating the applied shear to the particles in the layers below. We address this query by studying how the simultaneous application of constant strain shear and uniaxial compaction affects the evolution of the packing structure, and whether the structure of the shearing surface has any effect. We control the nature of the strain applying surface by generating a surface comprised of identical particles (similar to the bulk particles) arranged on a plane in different ordered and random spatial configurations.

The paper is subdivided into the following sections: section 2 provides a description of the sheared system we have explored; section 3 describes the details of the numerical model and the numerical experiment; section 4 presents our numerical results and section 5 summarizes the proceedings.

Existing work (Mueggenburg 2004)-(Tsai & Golub 2004) has addressed various aspects of shear-induced crystallization. One of the motivations behind this study has been to observe any crystallization or ordered packing which may arise from the simultaneous application of shear and uniaxial compaction by a surface comprised of particles constrained to a plane. Therefore, we have chosen a system of monodisperse Microcrystalline Cellulose (MCC) spheres of diameter $200 \mu\text{m}$, as our example system. The MCC spheres are contained in a 3D cell which has 2D periodic boundary conditions. The cell is bound by planes normal to the vertical which form the bounding surfaces. The bounding surfaces are comprised of particles which are identical in all respects to those in the bulk, which may be arranged in a lattice configuration, or randomly positioned, on a plane. The particles are initially allowed to settle under acceleration due to gravity, or gravity compaction (GC), for a fixed interval of time. This phase is followed by the simultaneous application of constant strain shear and uniaxial compaction by the upper bounding surface for a set interval of time. Our results indicate that the geometric characteristics, such as the packing fraction, the average coordination number, the radial distribution function, the distribution of contacts and contact angles, of the evolving particle packing are strongly influenced by the shear and compaction strain rates. In this paper we discuss our results for simulations carried out using 1800 MCC spheres confined between the bounding surfaces.

3 NUMERICAL MODEL

The numerical experiments are performed using the 3D Discrete Element Method (DEM) simulations (Cundall & Strack 1979). The particles are non-rigid spheres which can undergo small deformations upon contact with the other particles. The degree of deformation at a contact determines the contact force experienced by the two particles forming the contact which, according to Newton's Third Law, are equal and opposite to one another. We have used the Hertz-Kuwabara-Kono contact force model (Dutt, Hancock, Bentham & Elliott 2005) to represent the normal contact force interactions and, the linear damped harmonic oscillator model to represent the tangential contact force interactions. The material properties of MCC, such as the Young's modulus ($9.08 \times 10^9 \text{ Pa}$) and the Poisson ratio (0.3) (Alderborn & Nystrom 1996), are used to determine the contact force parameters. The particles forming the bounding surface and those in the bulk have identical material properties. We have included the effects of the interparticle substrate friction by adhering to the

Coulomb's friction criteria (Aastrom, Herrmann & Timonen 2000); thereby, adding two more control parameters: the coefficient of kinetic friction μ_k and the coefficient of static friction μ_{stat} . In our calculations, we have set $\mu_k = \mu_{stat} = 0.1$. As mentioned earlier, all the simulations are performed in two stages: the particles are allowed to settle under gravity followed by the simultaneous application of constant strain shear and uniaxial compaction, each phase is carried out for the same interval of time, for all the simulation runs. Further details of the interparticle forces and the numerical simulation can be found in (Dutt, Hancock, Bentham & Elliott 2005).

4 RESULTS

In this paper, we present our findings for systems where the bounding surfaces were generated by arranging the $200 \mu\text{m}$ diameter MCC spheres in a 2D square lattice configuration, unless specified otherwise.

In the particle packing problems, some of the macroscopic and microscopic indicators of the internal structure of the evolving dense particle agglomerates are the packing fraction, the average coordination number, the radial distribution function and the contact angle distributions. We have characterized the evolving internal structure under externally applied compaction and shear by computing these quantities. Fig. 1 shows the time evolution of the packing fraction for the various numerical experiments which have been carried out under the shear strain rate of $250 \mu\text{m/s}$ but different compaction strain rates, beginning from a time when most of the particles have settled. The packing fraction increases from 0 to 0.45 as the particles settle under acceleration due to gravity until time $t \approx 0.425 \text{ s}$, followed by the application of the uniaxial compaction and shear phase for a fixed interval of time. Since the particles are still in the process of settling, the packing fraction increases linearly for all the compaction strain rates till either the simulation completes the preset number of iterations, or the packing fraction attains a value in the vicinity of 0.53, as reinforced by Fig. 2. For example, the compaction strain rate of $1000 \mu\text{m/s}$ is sufficiently low so to allow the packing fraction to increase linearly until the simulation ends. There is significant rearrangement of the particles as the value of the packing fraction jumps from 0.53 to 0.6. The second phase of the linearity in the time rate of change of the packing fraction is observed for higher compaction strain rates. For ease of discussion, we subdivide the time evolution of the packing fraction into regions marked by different points: A denotes the point at which the packing fraction ceases to increase linearly with the externally applied strain, when the packing frac-

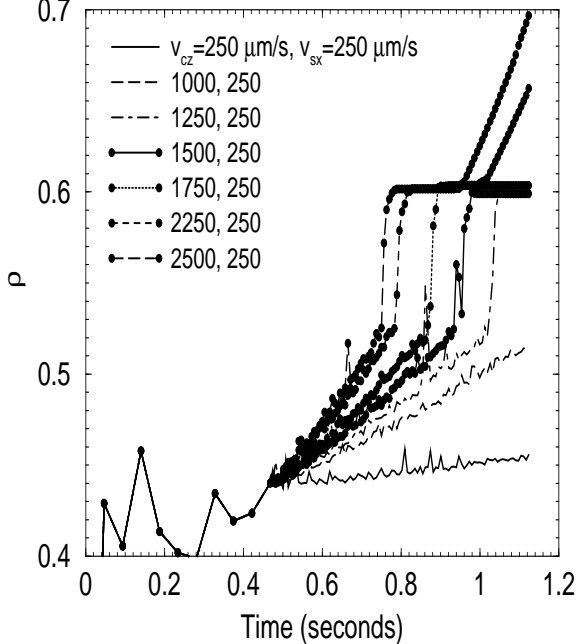


Figure 1. The time evolution of the packing fraction for different uniaxial compaction strain rates. The shear strain rate for all simulations was set at $250 \mu\text{m/s}$. In the legend, the first number represents the uniaxial compaction strain rate and the second number represents the shear strain rate; the units are $\mu\text{m/s}$.

tion fraction is approximately 0.53; B denotes the point which the packing fraction attains a value of 0.6 after a sharp transition from a value of 0.53, and C is the point at which either the simulation ends, or the packing fraction ceases to remain at a steady value of 0.6, and again begins to increase linearly with time. The jump in the packing fraction values from 0.53 to 0.6 is related to the transition of the particle packings to the random loose packing (RLP) state. This transition is found to

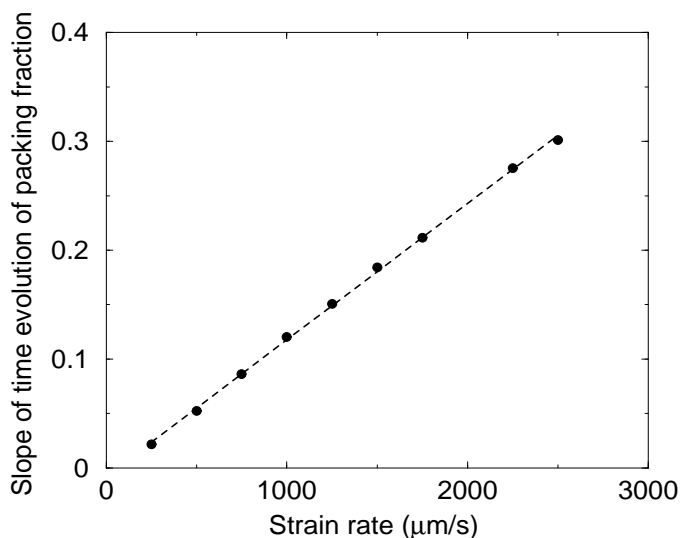


Figure 2. Slope of the time evolution of the packing fraction as a function of the compaction strain rate for a shear strain rate of $250 \mu\text{m/s}$. This measurement spans from the commencement of the simultaneous application of shear and compaction to point A, or the termination of the numerical experiment.

occur at increasingly delayed stages of the simulation with decreasing compaction strain rates. Figs. 3 and 4 show the azimuthal angle distribution and the radial distribution functions (RDFs), respectively, for instances of the individual simulations pertaining to the points A, B, C, and the final configuration of the various numerical experiments carried out at different compaction strain rates but the same shear strain rate of $250 \mu\text{m/s}$, as indicated in the figure legends. The azimuthal angle distribution looks at the angle made by the contact vector (the vector connecting the centers of mass of the two particle in contact) with the vertical. The RDF is indicative of close packing by the equal amplitudes of the second and third peaks (Clarke & Jonsson 1993); where as, the azimuthal angle distribution shows a preference for 45 degrees and 90 degrees. The latter arises from contacts between particles lying in a plane normal to the vertical, and the former arises from contacts between particles lying on a plane at 45 degrees to the vertical. This situation will occur for particles close to the top and the bottom bounding surfaces which have particles arranged in a square lattice. At point A where the packing fraction is low (~ 0.53), the ordered packing arises in the vicinity of the bottom surface; hence, resulting in the preferred orientation of 45 or 90 degrees. For a compaction strain rate of $1750 \mu\text{m/s}$, the simulation terminates before point C can be reached. This is a consequence of the transition to the RLP state which makes the strain applying surface lose contact with a large fraction of the particles on the surface of the agglomerate, therefore maintaining the packing fraction steady for a time interval of about 0.2 s. For higher values of the compaction strain rate, once the strain applying surface regains contact with a significant fraction of the particles, the packing fraction begins to again increase linearly, as seen for the compaction strain rates of $2250 \mu\text{m/s}$ and $2500 \mu\text{m/s}$. The RDF and the azimuthal angle distribution of the final configurations for the compaction strain rates of $2250 \mu\text{m/s}$ and $2500 \mu\text{m/s}$ (as shown in Figs. 3 and 4) show the development of long range order in the particle packings. Numerical experiments with smaller systems (900 MCC spheres with $200 \mu\text{m}$ diameter confined to the same dimensions) evolve into inter-digitating layers with a height of 5 particle diameters. On repeating our numerical experiments with different shear strain rates, we have found the results to be insensitive to the values of the shear strain rates which we have chosen so far. Our computations of the time evolution of the coordination number for each of the numerical experiments strongly highlights the dominance of the compaction strain rate over the shear strain rate in determining the dynamics and therefore, the evolu-

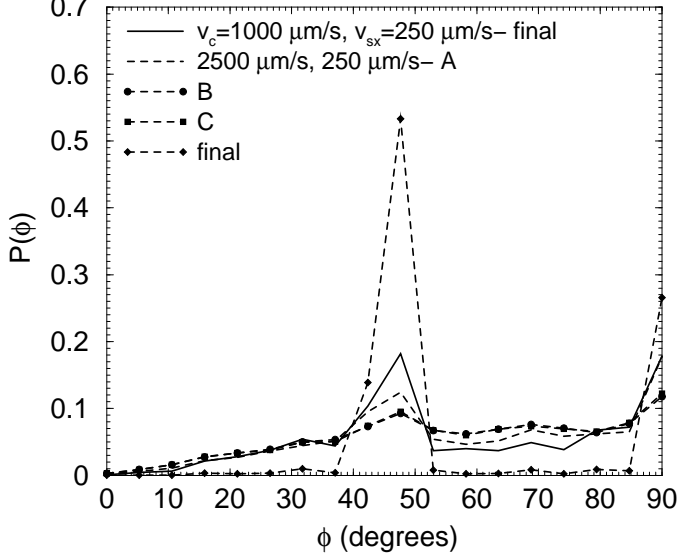


Figure 3. The distribution of the azimuthal angles ϕ for the various instances of the different numerical experiments performed under the same shear strain rate (the second number in the legend) but at two compaction strain rates (indicated by the first number in the legend).

tion of the packing structure. Other characteristics of the packing structure have demonstrated similar findings. We have also varied the initial height of the agglomerate of particles after settling under gravity but before the commencement of the shear and compaction phase by adjusting the initial average kinetic energy of the particles. We find these variations to yield very similar results to what has been presented above. Our preliminary studies using bounding surfaces with the particles arranged randomly or in a triangular lattice have yielded similar trends in the behavior of the packing characteristics described earlier. We will present these results along with other details of the current work in future publications.

5 DISCUSSIONS

Our findings for simultaneously sheared and compacted systems show an evolution to an ordered packing state which occurs at increasingly earlier stages of the numerical experiment with increasing compaction strain rate. The packing structure has been found to change from a random loose packing to a random close packing and finally, to a more ordered configuration, as shown above. Observations of these phases in our numerical experiments depends upon the strain rates and the duration of the simulation.

We would like to acknowledge Pfizer for providing funding support.

REFERENCES

- Åström, J.A., Herrmann, H.J. and Timonen, J. 2000, Granular packings and faults, *Phys. Rev. Lett.* 84 638.
- Pharmaceutical Powder Compaction Technology, Marcel Dekker Inc., New York 1996, Ed. Goran Alderborn and Christer Nyström.

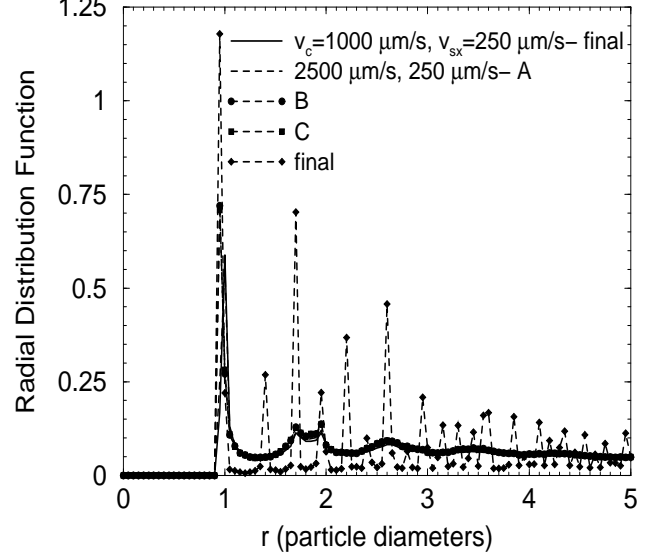


Figure 4. Radial distribution function calculations for the various instances of the different numerical experiments. In the legend, the first number represents the uniaxial compaction strain rate and the second number represents the shear strain rate.

- Clarke, A.S. and Jonsson, H. 1993, Structural changes accompanying densification of random hard-sphere packings, *Phys. Rev. E* 47 3975.
- Cundall, P.A. and Strack, O.D.L., A discrete numerical model for granular assemblies, *Géotechnique* 29 47.
- Dutt, M., Hancock, B., Bentham, C. and Elliott, J. 2005, An implementation of granular dynamics for simulating frictional elastic particles based on the DL_POLY code, *Comp. Phys. Comm.* 166 26.
- Jaeger, H.M., Nagel, S.R. Nagel, and Behringer, R.P. 1996, Granular solids, liquids and gases, *Rev. Mod. Phys.* 68 1259.
- Liu, C.-h., Nagel, S.R., Schecter, D.A., Majumdar, S.N., Narayan, O. and Witten, T.A. 1995, Force fluctuations in bead packs, *Science* 269 513.
- Richard, P., Philippe, P., Barbe, F., Bourles, S., Thibault, X. and Bideau, D. 2003, Analysis by x-ray microtomography of a granular packing undergoing compaction, *Phys. Rev. E* 68 020301.
- Schäfer, J., Dippel, S. and Wolf, D.E. 1996, Force schemes in simulations of granular materials, *J. Phys. I France* 6 5.
- Silbert, L.E., Ertas, D.E., Grest, G.S., Halsey, T.C. and Levine, D. 2002, Geometry of frictionless and frictional sphere packings, *Phys. Rev. E* 65 031304.
- Thornton, C. and Anthony, S.J. 1998, Quasi-static deformation of particulate media, *Phil. Trans. R. Soc. Lond. A* 356 2763.
- Tsai, J.-C., Voth, G.A. and Gollub, J.P. 2003, Internal granular dynamics, shear-induced crystallization, and compaction steps, *Phys. Rev. Lett.* 91 064301.
- Tsai, J.-C. and Gollub, J.P. 2004, Slowly sheared dense granular flows: crystallization and nonunique final states, *Phys. Rev. E* 70, 031303.
- Mueggenburg, N.W. 2004, The behavior of granular materials under cyclic shear, cond-mat/0408010.